4. DIFFUSE SCATTERING AND RELATED TOPICS
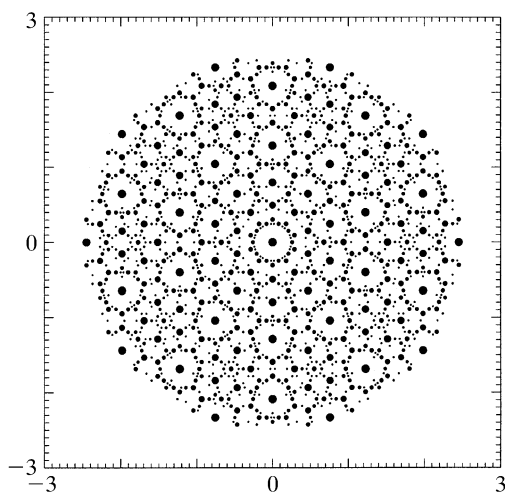

Fig. 4.6.3.17. Schematic diffraction pattern of the Penrose tiling (edge length of the Penrose unit rhombs $a_r = 4.04$ Å). All reflections are shown within $10^{-2}|F(\mathbf{0})|^2 < |F(\mathbf{H})|^2 < |F(\mathbf{0})|^2$ and $0 \le |\mathbf{H}^{\parallel}| \le 2.5$ Å^{-1}.
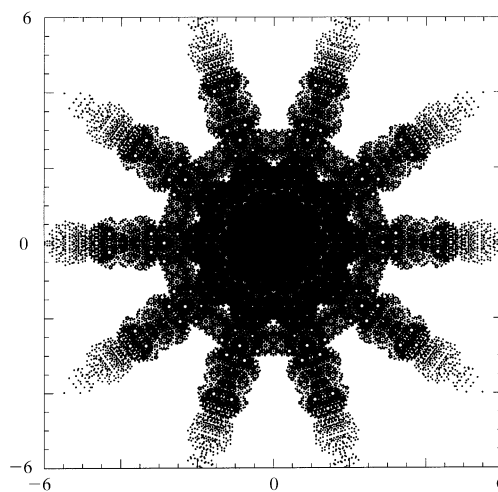

Fig. 4.6.3.19. The perpendicular-space diffraction pattern of the Penrose tiling (edge length of the Penrose unit rhombs $a_r = 4.04$ Å). All reflections are shown within $10^{-4}|F(\mathbf{0})|^2 < |F(\mathbf{H})|^2 < |F(\mathbf{0})|^2$ and $0 \le |\mathbf{H}^{\parallel}| \le 2.5$ Å^{-1}.

$M^* = M_1^* \oplus M_2^*$. $M_1^* = \{h_1\mathbf{a}_1^* + h_2\mathbf{a}_2^* + h_3\mathbf{a}_3^* + h_4\mathbf{a}_4^*\}$ corresponds to a $\mathbb{Z}$ module of rank 4 in a 2D subspace, $M_2^* = \{h_5\mathbf{a}_5^*\}$ corresponds to a $\mathbb{Z}$ module of rank 1 in a 1D subspace. Consequently, the first submodule can be considered as a projection from a 4D reciprocal lattice, $M_1^* = \pi^{\parallel}(\Sigma^*)$, while the second submodule is of the form of a regular 1D reciprocal lattice, $M_2^* = \Lambda^*$. The diffraction pattern of the Penrose tiling decorated with equal point scatterers on its vertices is shown in Fig. 4.6.3.17. All Bragg reflections within $10^{-2}|F(\mathbf{0})|^2 < |F(\mathbf{H})|^2 < |F(\mathbf{0})|^2$ are depicted. Without intensity-truncation limit, the diffraction pattern would be densely filled with discrete Bragg reflections. To illustrate their spatial and intensity distribution, an enlarged section of Fig. 4.6.3.17 is shown in Fig. 4.6.3.18. This picture shows all Bragg reflections within $10^{-4}|F(\mathbf{0})|^2 < |F(\mathbf{H})|^2 < |F(\mathbf{0})|^2$. The projected 4D reciprocal-lattice unit cell is drawn and several reflections are indexed. All reflections are arranged along lines in five symmetry-equivalent orientations. The perpendicular-space diffraction patterns (Figs. 4.6.3.19 and 4.6.3.20) show a characteristic star-like distribution of the Bragg reflections. This is a consequence of the pentagonal shape of the atomic surfaces: the Fourier transform of a pentagon has a star-like distribution of strong Fourier coefficients.

The 5D decagonal space groups that may be of relevance for the description of decagonal phases are listed in Table 4.6.3.1. These space groups are a subset of all 5D decagonal space groups fulfilling the condition that the 5D point groups they are associated with are isomorphous to the 3D point groups describing the diffraction symmetry. Their structures are comparable to 3D hexagonal groups. Hence, only primitive lattices exist. The orientation of the symmetry elements in the 5D space is defined by the isomorphism of the 3D and 5D point groups. However, the action of the tenfold rotation is different in the subspaces $V^{\parallel}$ and $V^{\perp}$: a rotation of $\pi/5$ in $V^{\parallel}$ is correlated with a rotation of $3\pi/5$ in $V^{\perp}$. The reflection and inversion operations are equivalent in both subspaces.

4.6.3.3.2.3. *Structure factor*

The structure factor for the decagonal phase corresponds to the Fourier transform of the 5D unit cell,
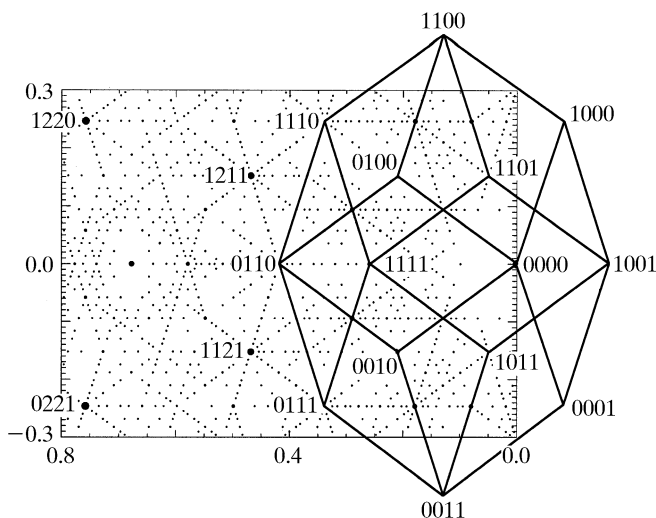

Fig. 4.6.3.18. Enlarged section of Fig. 4.6.3.17. All reflections shown are selected within the given limits from a data set within $10^{-4}|F(\mathbf{0})|^2 < |F(\mathbf{H})|^2 < |F(\mathbf{0})|^2$ and $0 \le |\mathbf{H}^{\parallel}| \le 2.5$ Å^{-1}. The projected 4D reciprocal-lattice unit cell is drawn and several reflections are indexed.
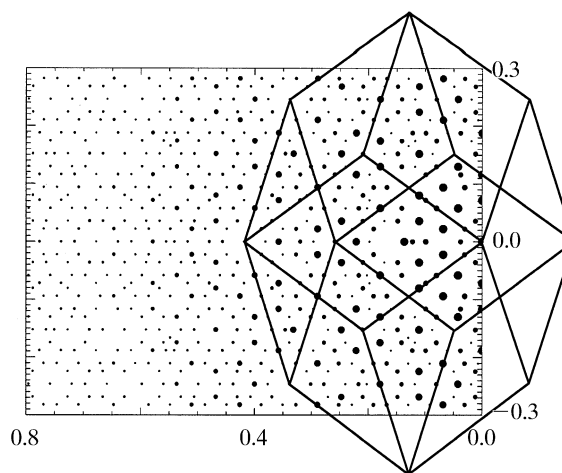

Fig. 4.6.3.20. Enlarged section of Fig. 4.6.3.19 showing the projected 4D reciprocal-lattice unit cell.

506

Table 4.6.3.1. *3D point groups of order k describing the diffraction symmetry and corresponding 5D decagonal space groups with reflection conditions (see Rabson et al., 1991)*

3D point group	k	5D space group	Reflection condition
$\dfrac{10}{m}\dfrac{2}{m}\dfrac{2}{m}$	40	$P\dfrac{10}{m}\dfrac{2}{m}\dfrac{2}{m}$	No condition
		$P\dfrac{10}{m}\dfrac{2}{c}\dfrac{2}{c}$	$h_1h_2h_2h_1h_5 : h_5 = 2n$ $h_1h_2\overline{h_2h_1}h_5 : h_5 = 2n$
		$P\dfrac{10_5}{m}\dfrac{2}{m}\dfrac{2}{c}$	$h_1h_2\overline{h_2h_1}h_5 : h_5 = 2n$
		$P\dfrac{10_5}{m}\dfrac{2}{c}\dfrac{2}{m}$	$h_1h_2h_2h_1h_5 : h_5 = 2n$
$\dfrac{10}{m}$	20	$P\dfrac{10}{m}$	No condition
		$P\dfrac{10_5}{m}$	$0000h_5 : h_5 = 2n$
1022	20	$P1022$	No condition
		$P10_j22$	$0000h_5 : jh_5 = 10n$
$10mm$	20	$P10mm$	No condition
		$P10cc$	$h_1h_2h_2h_1h_5 : h_5 = 2n$ $h_1h_2\overline{h_2h_1}h_5 : h_5 = 2n$
		$P10_5mc$	$h_1h_2\overline{h_2h_1}h_5 : h_5 = 2n$
		$P10_5cm$	$h_1h_2h_2h_1h_5 : h_5 = 2n$
$\overline{10}m2$	20	$P\overline{10}m2$	No condition
		$P\overline{10}c2$	$h_1h_2h_2h_1h_5 : h_5 = 2n$
		$P\overline{10}2m$	No condition
		$P\overline{10}2c$	$h_1h_2\overline{h_2h_1}h_5 : h_5 = 2n$
10	10	$P10$	No condition
		$P10_j$	$0000h_5 : jh_5 = 10n$

$$F(\mathbf{H}) = \sum_{k=1}^{N} f_k(\mathbf{H}^{\parallel})T_k(\mathbf{H}^{\parallel},\mathbf{H}^{\perp})g_k(\mathbf{H}^{\perp})\exp(2\pi i\mathbf{H}\cdot\mathbf{r}_k),$$

with 5D diffraction vectors $\mathbf{H} = \sum_{i=1}^{5} h_i\mathbf{d}_i^*$, N hyperatoms, parallel-space atomic scattering factor $f_k(\mathbf{H}^{\parallel})$, temperature factor $T_k(\mathbf{H}^{\parallel},\mathbf{H}^{\perp})$ and perpendicular-space geometric form factor $g_k(\mathbf{H}^{\perp})$. $T_k(\mathbf{H}^{\parallel},\mathbf{0})$ is equivalent to the conventional Debye–Waller factor and $T_k(\mathbf{0},\mathbf{H}^{\perp})$ describes random fluctuations along the perpendicular-space coordinate. These fluctuations cause characteristic jumps of vertices in physical space (*phason flips*). Even random phason flips map the vertices onto positions which can still be described by physical-space vectors of the type $\mathbf{r} = \sum_{i=1}^{5} n_i\mathbf{a}_i$. Consequently, the set $M = \{\mathbf{r} = \sum_{i=1}^{5} n_i\mathbf{a}_i | n_i \in \mathbb{Z}\}$ of all possible vectors forms a $\mathbb{Z}$ module. The shape of the atomic surfaces corresponds to a selection rule for the positions actually occupied. The geometric form factor $g_k(\mathbf{H}^{\perp})$ is equivalent to the Fourier transform of the *atomic surface*, i.e. the 2D perpendicular-space component of the 5D *hyperatoms*.

For example, the canonical Penrose tiling $g_k(\mathbf{H}^{\perp})$ corresponds to the Fourier transform of pentagonal atomic surfaces:

$$g_k(\mathbf{H}^{\perp}) = (1/A_{\mathrm{UC}}^{\perp})\int_{A_k} \exp(2\pi i\mathbf{H}^{\perp}\cdot\mathbf{r})\,\mathrm{d}\mathbf{r},$$

where $A_{\mathrm{UC}}^{\perp}$ is the area of the 5D unit cell projected upon $\mathbf{V}^{\perp}$ and A_k is the area of the kth atomic surface. The area $A_{\mathrm{UC}}^{\perp}$ can be calculated using the formula

$$A_{\mathrm{UC}}^{\perp} = (4/25a_i^{*2})[(7+\tau)\sin(2\pi/5) + (2+\tau)\sin(4\pi/5)].$$

Evaluating the integral by decomposing the pentagons into triangles, one obtains

$$g_k(\mathbf{H}^{\perp}) = \frac{1}{A_{\mathrm{UC}}^{\perp}}\sin\left(\frac{2\pi}{5}\right)$$
$$\times \sum_{j=0}^{4} \frac{A_j[\exp(iA_{j+1}\lambda_k) - 1] - A_{j+1}[\exp(iA_j\lambda_k) - 1]}{A_jA_{j+1}(A_j - A_{j+1})}$$

with $j = 0, \ldots, 4$ running over the five triangles, where the radii of the pentagons are λ_j, $A_j = 2\pi\mathbf{H}^{\perp}\mathbf{e}_j$,

$$\mathbf{H}^{\perp} = \pi^{\perp}(\mathbf{H}) = \sum_{j=0}^{4} h_j a_j^* \begin{pmatrix} 0 \\ 0 \\ 0 \\ \cos(6\pi j/5) \\ \sin(6\pi j/5) \end{pmatrix}$$

and the vectors

$$\mathbf{e}_j = \frac{1}{a_j^*} \begin{pmatrix} 0 \\ 0 \\ 0 \\ \cos(2\pi j/5) \\ \sin(2\pi j/5) \end{pmatrix} \text{ with } j = 0, \ldots, 4.$$

As shown by Ishihara & Yamamoto (1988), the Penrose tiling can be considered to be a superstructure of a pentagonal tiling with only one type of pentagonal atomic surface in the nD unit cell. Thus, for the Penrose tiling, three special reflection classes can be distinguished: for $|\sum_{i=1}^{4} h_i| = m$ mod 5 and $m = 0$ the class of strong main reflections is obtained, and for $m = \pm1, \pm 2$ the classes of weaker first- and second-order satellite reflections are obtained (see Fig. 4.6.3.18).

4.6.3.3.2.4. *Intensity statistics*

This section deals with the reciprocal-space characteristics of the 2D quasiperiodic component of the 3D structure, namely the Fourier module M_1^*. The radial structure-factor distributions of the Penrose tiling decorated with point scatterers are plotted in Figs. 4.6.3.21 and 4.6.3.22 as a function of parallel and perpendicular space. The distribution of $|F(\mathbf{H})|$ as a function of their frequencies clearly resembles a centric distribution, as can be expected from the centrosymmetric 4D subunit cell. The shape of the distribution function depends on the radius of the limiting sphere in reciprocal space. The number of weak reflections increases to the power of four, that of strong reflections only quadratically (strong reflections always have small $\mathbf{H}^{\perp}$ components). The radial distribution of the structure-factor amplitudes as a function of perpendicular space clearly shows three branches, corresponding to the reflection classes $\sum_{i=1}^{4} h_i = m$ mod 5 with $|m| = 0$, $|m| = 1$ and $|m| = 2$ (Fig. 4.6.3.23).

The weighted reciprocal space of the Penrose tiling contains an infinite number of Bragg reflections within a limited region of the physical space. Contrary to the diffraction pattern of a periodic structure consisting of point atoms on the lattice nodes, the Bragg reflections show intensities depending on the perpendicular-space components of their diffraction vectors (Figs. 4.6.3.19, 4.6.3.20 and 4.6.3.22).

references